



## Open Research Online

---

The Open University's repository of research publications  
and other research outputs

# Skeletal muscle stem cells express anti-apoptotic ErbB receptors during activation from quiescence

## Journal Article

How to cite:

Golding, Jon P; Calderbank, Emma; Partridge, Terence and Beauchamp, Jonathan (2007). Skeletal muscle stem cells express anti-apoptotic ErbB receptors during activation from quiescence. *Experimental Cell Research*, 313(2), pp. 341-356.

For guidance on citations see [FAQs](#).

© [\[not recorded\]](#)

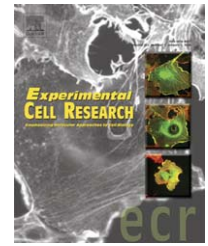
Version: [\[not recorded\]](#)

Link(s) to article on publisher's website:  
<http://dx.doi.org/doi:10.1016/j.yexcr.2006.10.019>

---

Copyright and Moral Rights for the articles on this site are retained by the individual authors and/or other copyright owners. For more information on Open Research Online's data [policy](#) on reuse of materials please consult the policies page.

---

available at [www.sciencedirect.com](http://www.sciencedirect.com)[www.elsevier.com/locate/yexcr](http://www.elsevier.com/locate/yexcr)

## Research Article

# Skeletal muscle stem cells express anti-apoptotic ErbB receptors during activation from quiescence

Jon P. Golding<sup>a,\*</sup>, Emma Calderbank<sup>b</sup>, Terence A. Partridge<sup>b</sup>, Jonathan R. Beauchamp<sup>b</sup>

<sup>a</sup>Department of Biological Sciences, Open University, Walton Hall, Milton Keynes, MK7 6AA, UK

<sup>b</sup>Muscle Cell Biology Group, Medical Research Council Clinical Sciences Centre, Faculty of Medicine, Imperial College, Hammersmith Hospital Campus, Du Cane Road, London, W12 0NN, UK

### ARTICLE INFORMATION

#### Article Chronology:

Received 4 May 2006

Revised version received

9 October 2006

Accepted 16 October 2006

#### Keywords:

Muscle stem cell

Satellite cell

Apoptosis

Activation

erbB

EGFr

### ABSTRACT

To be effective for tissue repair, satellite cells (the stem cells of adult muscle) must survive the initial activation from quiescence. Using an in vitro model of satellite cell activation, we show that erbB1, erbB2 and erbB3, members of the EGF receptor tyrosine kinase family, appear on satellite cells within 6 h of activation. We show that signalling via erbB2 provides an anti-apoptotic survival mechanism for satellite cells during the first 24 h, as they progress to a proliferative state. Inhibition of erbB2 signalling with AG825 reduced satellite cell numbers, concomitant with elevated caspase-8 activation and TUNEL labelling of apoptotic satellite cells. In serum-free conditions, satellite cell apoptosis could be largely prevented by a mixture of erbB1, erbB3 and erbB4 ligand growth factors, but not by neuregulin alone (erbB3/erbB4 ligand). Furthermore, using inhibitors specific to discrete intracellular signalling pathways, we identify MEK as a pro-apoptotic mediator, and the erbB-regulated factor STAT3 as an anti-apoptotic mediator during satellite cell activation. These results implicate erbB2 signalling in the preservation of a full complement of satellite cells as they activate in the context of a damaged muscle.

© 2006 Elsevier Inc. All rights reserved.

## Introduction

Satellite cells, a population of undifferentiated tissue-specific stem cells, comprise only about 2% of the total nuclei of normal adult skeletal muscle [1–3]. Despite this apparently small reserve of potentially proliferative cells, skeletal muscle nevertheless exhibits an astonishing regenerative capacity, with each satellite cell able to generate several thousand new myonuclei [3] on a time scale that allows total replacement of the parent myofibre within 4 days of injury [4]. Because of their fundamental role in muscle regeneration, robust mechanisms must exist to assure the survival of satellite cells within the context of a damaged muscle. Once activated from quies-

cence, the amplifying progeny of satellite cells (myoblasts) are sensitive to apoptotic cell death as they proliferate [5,6] and differentiate [7,8]. However, the sensitivity of satellite cells to apoptotic death during the activation process, within the first 24 h following myotrauma, has not been determined. This is a critical period during muscle regeneration, during which satellite cells undergo an important series of molecular changes prior to cell division [9–11], while at the same time having to adjust to the physiological stresses of muscle injury.

In response to myotrauma, intracellular reactive oxygen species (ROS) are generated [12–14]. ROS is a key effector of death in most cells [15] and of DNA damage in myoblasts [16], while under conditions of transient oxidative stress, human

\* Corresponding author. Fax: +44 1908 654167.

E-mail address: [j.p.golding@open.ac.uk](mailto:j.p.golding@open.ac.uk) (J.P. Golding).

68 satellite cells show decreased viability and become non-  
69 proliferative [17]. Under normal conditions, catalase and  
70 glutathione transferase antioxidants expressed by quiescent  
71 satellite cells can protect against ROS [18]. However, these  
72 defence systems become overwhelmed by excessive ROS  
73 production, as occurs following injury and in various pathol-  
74 ogies [19], highlighting the potential vulnerability of satellite  
75 cells to apoptosis following myotrauma. During the late  
76 regenerative phase, as myoblasts exit the cell cycle and  
77 differentiate, anti-apoptotic signals are transduced by two  
78 members of the erbB family of receptor tyrosine kinases: erbB1  
79 (the EGF receptor) [20] and erbB2 [21], raising the possibility  
80 that these erbB receptors might also provide anti-apoptotic  
81 signals, during satellite cell activation.

82 The erbB family comprises erbB1, erbB2, erbB3 and erbB4  
83 [22], while the metalloendopeptidase *N*-arginine dibasic con-  
84 vertase (NRDc) binds heparin-binding EGF-like growth factor  
85 and thereby acts as a co-receptor with erbB1 [23]. Ligand  
86 binding causes erbB receptors to dimerise and phosphorylate,  
87 with erbB2 being the preferred dimerisation partner of the  
88 other erbB receptors, although erbB2 itself has no known  
89 ligand [22]. ErbB receptors are expressed by many cell types  
90 and regulate diverse cellular functions that include prolifera-  
91 tion, migration, cell fate decisions, differentiation and apop-  
92 tosis [22,24]. In normal, undamaged skeletal muscle, erbB2,  
93 erbB3 and erbB4 receptors are exclusively localised to the  
94 neuromuscular junction (NMJ) [25,26], where they regulate the  
95 expression of acetylcholine receptors [27,28] and glucose  
96 transport within myofibres [29]. Although NRDc is highly  
97 expressed by human skeletal muscle [30], its cellular localisa-  
98 tion has not been determined. In tissue culture models of the  
99 late phase of muscle injury, myoblasts express erbB1, erbB2  
100 and erbB3 receptors [21,31–33], as they commit to differentia-  
101 tion. However, it remains unknown whether erbB receptors  
102 are expressed by satellite cells and if so, at which stage of the  
103 activation process they first appear and how their expression  
104 is regulated.

105 In this study, we show that satellite cells do not  
106 express any erbB receptors in the quiescent state. How-  
107 ever, erbB1, erbB2 and erbB3 become expressed within 6 h  
108 of activation, while erbB4 and NRDc can be detected  
109 within 24 h. We demonstrate that erbB2 signalling plays  
110 an anti-apoptotic role in preserving the full complement  
111 of satellite cells during this critical phase of stem cell  
112 activation from quiescence.

## 113 Materials and methods

### 115 Animals

116 C57Bl/10 mice, myosin light chain 3F-nLacZ-2E (MLC-3F<sup>nLacZ</sup>)  
117 mice [34] and Myf5<sup>nLacZ/+</sup> mice [35], aged between 6 and  
118 8 weeks, were from breeding colonies maintained at MRC  
119 Hammersmith.

### 120 Tissue preparation and single myofibre isolation

121 Entire extensor digitorum longus (EDL) and tibialis anterior (TA)  
122 muscles were removed. The TAs were snap frozen for

123 cryosectioning and the EDLs were dissociated into single  
124 muscle fibres (myofibres), as described previously [36].

### Myofibre culture

125 Isolated myofibres were maintained as non-adherent cul-  
126 tures in DMEM, containing 10% horse serum (PAA Labora-  
127 tories) and 0.5% chick embryo extract (ICN Flow) as  
128 described previously [36]. Myofibres were subsequently  
129 fixed with 4% paraformaldehyde in PBS (4% PAF) for  
130 20 min prior to immunostaining. 131

### Growth factors

132 Recombinant Human EGF, HB-EGF and NRG (NRG-1  $\beta$ 1 EGF  
133 domain) were obtained from R&D Systems. 134

### ErbB inhibitors

135 The erbB1-selective inhibitor AG1478 (Calbiochem) was  
136 dissolved in DMSO and used at a 1:500 dilution to give a  
137 10- $\mu$ M working concentration (autophosphorylation: erbB1  
138 IC<sub>50</sub>=0.003 $\mu$ M; erbB2 IC<sub>50</sub>>100  $\mu$ M [37]). The erbB2-selective  
139 inhibitor AG825 (Calbiochem) was dissolved in DMSO and  
140 used at a 1:500 dilution to give a 50- $\mu$ M working  
141 concentration (autophosphorylation: erbB2 IC<sub>50</sub>=0.35  $\mu$ M;  
142 erbB1 IC<sub>50</sub>=19  $\mu$ M. Substrate phosphorylation: erbB2 IC<sub>50</sub>=  
143 9.5  $\mu$ M; erbB1 IC<sub>50</sub>>100  $\mu$ M [38]). Control cultures contained  
144 1:500 DMSO. 145

### Signal transduction pathway-specific inhibitors

146 All inhibitors were obtained from Calbiochem and were  
147 dissolved in DMSO, unless stated otherwise. The following  
148 inhibitors were used at the working concentrations shown  
149 (typically 1000-fold dilutions of the stock solution): Akt inhi-  
150 bitor, 10  $\mu$ M (Akt IC<sub>50</sub>=5  $\mu$ M). U0126, MEK1/2 inhibitor, 12.5  $\mu$ M  
151 (MEK1 IC<sub>50</sub>=72 nM, MEK2 IC<sub>50</sub>=58 nM). Jnk inhibitor II, 20  $\mu$ M  
152 (Jnk-1/Jnk-2 IC<sub>50</sub>=40 nM, Jnk-3 IC<sub>50</sub>=90 nM). SB203580,  
153 p38MAP-K inhibitor, 2  $\mu$ M (p38MAP-K IC<sub>50</sub>= 600 nM). U-73122,  
154 PLC $\gamma$  inhibitor, 5  $\mu$ M (PLC IC<sub>50</sub>=2  $\mu$ M). IC<sub>50</sub> values are quoted  
155 from the product data sheets. Caspase-8 competitive inhibitor  
156 I, cell-permeable, 100 nM [39]. STAT3 inhibitor, cell-permeable,  
157 1 mM (solid dissolved directly in culture medium to working  
158 concentration, immediately prior to use) [40]. 159

### Histology

160 Cultured myofibres from MLC-3F<sup>nLacZ</sup> mice and TA muscle  
161 cryosections from Myf5<sup>nLacZ/+</sup> mice were fixed in 4% PAF for  
162 5 min.  $\beta$ -Galactosidase activity was visualised by incubation in  
163 4 mM potassium ferrocyanide, 4 mM potassium ferricyanide,  
164 2 mM MgCl<sub>2</sub>, 400  $\mu$ g/ml X-gal, 0.02% NP40 in PBS for 10 min at  
165 37°C. Myofibres were then washed in PBS and processed for  
166 immunohistochemistry. 167

### Immunostaining

168 Fixed myofibres were permeabilised with 0.5% Triton X-100/  
169 PBS for 10 min. Cryosections were fixed in 4% PAF for 10 min  
170

171 and washed in PBS. Non-specific antibody binding was  
172 blocked by incubation in 20% goat serum in PBS for 30 min.

173 Rabbit anti-erbB2 (sc-284, Santa Cruz, 1:200 dilution,  
174 1 µg/ml working conc.) and rabbit anti-erbB4 (06-572,  
175 Upstate, 1:100, 10 µg/ml working conc.) antibodies have  
176 been previously characterised on rodent skeletal muscle  
177 sections [26], while mouse anti-erbB3 antibody (Ab-5,  
178 Calbiochem, 1:100, 2 µg/ml working conc.) has been  
179 previously characterised on L6 and C2C12 rodent skeletal  
180 muscle cell lines [33]. Other primary antibodies were mouse  
181 anti-erbB1 (clone 13, BD Bioscience, 1:20, 12.5 µg/ml working  
182 concentration); mouse anti-Pax7 (Developmental Studies  
183 Hybridoma Bank, 1:10); rabbit anti-MyoD (sc-760, Santa  
184 Cruz, 1:80); mouse anti-MyoD1 (clone 5.8A, DakoCytoma-  
185 tion, 1:80); mouse anti-myogenin (clone F5D, Developmental  
186 Studies Hybridoma Bank, 1:80); rabbit anti-NRDc (gift of  
187 Annik Prat, Institut de Recherches Cliniques de Montreal,  
188 1:400); rat anti-BrdU (Abcam, 1:500, used as in [10]); rabbit  
189 anti-phospho(Tyr877)-erbB2 and rabbit anti-phospho  
190 (Tyr1248)-erbB2 (Cell Signalling Technology, used together  
191 at 1:50); rabbit anti-phospho(Tyr1173)-erbB1 (ab5652, Abcam,  
192 1:100). Control mouse and rabbit IgG were used in place of  
193 primary antibodies at 10 µg/ml.

194 Primary antibodies were applied overnight at 4°C and  
195 then visualised by 2 h incubation with Alexa Fluor-con-  
196 jugated secondary antibodies (Molecular Probes, 1:200).  
197 Where indicated, Texas Red-conjugated α-bungarotoxin  
198 (Molecular probes, 1:1000) was mixed with the secondary  
199 antibody.

200 Immunostaining with antibodies against phosphorylated  
201 erbBs was carried out as above, except all solutions contained  
202 100 mM sodium orthovanadate. For de-phosphorylation  
203 controls, permeabilised myofibres were incubated with 6 U/  
204 ml alkaline phosphatase (Promega) in PBS pH8, without  
205 orthovanadate, for 2 h at 37°C before proceeding with serum  
206 blocking and primary antibodies.

207 Myofibres were mounted in Faramount (DakoCytomation)  
208 containing either 100 ng/ml 1,4-diazobicyclo[2,2,2]octane  
209 (DAPI) or 10 µg/ml propidium iodide. Conventional epifluo-  
210 rescence microscopy was performed with a Zeiss Axiophot  
211 microscope. Images were captured with a CCD-1300-Y camera  
212 (Princeton Instruments) and processed with Metamorph soft-  
213 ware (4.5r5 Universal Imaging). Confocal microscopy was  
214 performed with a Leica TCS-NT confocal microscope, using a  
215 Leica PL APO 100×/1.40-0.70 oil-immersion objective. Optical  
216 sections were recorded in 0.4 µm increments using sequential  
217 capture of double immunostains.

### 218 Caspase assay

219 Cultured myofibres were fixed in 4% PAF for 5 min and  
220 permeabilised for 10 min with 0.1% CHAPS and 2 mM EDTA  
221 in Ca<sup>2+</sup>/Mg<sup>2+</sup>-free PBS. Myofibres were washed in 2 mM EDTA in  
222 Ca<sup>2+</sup>/Mg<sup>2+</sup>-free PBS and then incubated with 0.25 mM fluoro-  
223 genic caspase-8 substrate: rhodamine 110, bis-(N-CBZ-L-iso-  
224 leucyl-L-glutamyl-L-threonyl-L-aspartic acid amide) (Molecular  
225 Probes) in 2 mM EDTA in Ca<sup>2+</sup>/Mg<sup>2+</sup>-free PBS for 30 min at 37°C.  
226 Myofibres were washed in 0.025% Tween20 in PBS, mounted  
227 without coverslip in 20% glycerol and viewed immediately on  
228 an epifluorescence microscope using a fluorescein filter set.

Myofibres were subsequently processed for Pax7 or MyoD 229  
immunofluorescence. 230

### TUNEL assay 231

Cultured myofibres were fixed in 4% PAF for 30 min, washed 232  
in PBS and then processed with TACS TdT fluorescein 233  
according to the manufacturer's protocols (R&D Systems). 234  
Stained myofibres were subsequently processed for Pax7 235  
immunofluorescence. 236

### Cell counting and statistics 237

The numbers of immunopositive cells per myofibre were 238  
counted by varying the focal plane at each point along the 239  
myofibre and are shown as the mean value ± SEM. Statistical 240  
differences between pairs of samples were assessed by 241  
unpaired 2-tailed Student's t-test. Statistical differences 242  
between multiple samples were assessed by Kruskal-Wallis 243  
non-parametric ANOVA with Dunn's post-test (GraphPad 244  
InStat 3.0a software). 245

## Results 246

### Localisation of erbB receptors in uninjured skeletal muscle 248

In sections of C57Bl/10 TA muscles, strong erbB1 immunor- 249  
eactivity was observed at the neuromuscular junction (NMJ, Fig. 250  
1A), identified by co-staining with α-bungarotoxin (Fig. 1A'). 251  
ErbB1 was also present generally on the surface of muscle 252  
fibres, connective tissue and capillaries (arrowhead and 253  
arrow, respectively in Fig. 1A). In agreement with previous 254  
studies [25,26] erbB2, erbB3 and erbB4 receptors were detected 255  
at the NMJ (Figs. 1B–D'). ErbB2 and erbB3 were additionally 256  
present on vasculature and connective tissues (Figs. 1B, C), in 257  
agreement with a previous study in rat [41]. Only erbB4 was 258  
present exclusively at NMJs (Fig. 1D'). NRDC was also localised 259  
predominantly to the NMJ (Fig. 1E'). However, towards the 260  
centre of the NMJ, NRDC immunostaining extended deep to 261  
the myofibre by an estimated 3–4 µm (arrowhead in Fig. 1E'). 262  
In addition, a subset of muscle fibres exhibited uniform NRDC 263  
immunoreactivity (asterisks in Fig. 1E), perhaps indicating 264  
differential expression in particular fibre types. In order to 265  
determine whether quiescent satellite cells expressed any 266  
erbB receptors, we used cryosections of EDL muscles from the 267  
Myf5<sup>nLacZ/+</sup> transgenic mouse, in which β-galactosidase is 268  
expressed by quiescent satellite cells [42]. Staining with X-gal 269  
identified satellite cell nuclei (blue dye reaction product 270  
marked with arrowheads in Figs. 1H–N). Co-immunofluores- 271  
cence staining revealed that none of the receptors were de- 272  
tectable on quiescent satellite cells (Figs. 1H'–L'). DAPI 273  
staining confirmed the location of satellite cell nuclei, 274  
although DAPI fluorescence is masked where the X-gal reac- 275  
tion product is particularly intense at the thickest, central 276  
region of the nucleus (merged antibody/DAPI shown in Figs. 277  
1H'–L'). Importantly, DAPI can still be detected in a ring at 278  
the periphery of the nucleus. Thus, X-gal does not mask any 279  
fluorescence from the satellite cell cytoplasm or cell surface, 280  
where erbB receptors would be located. 281

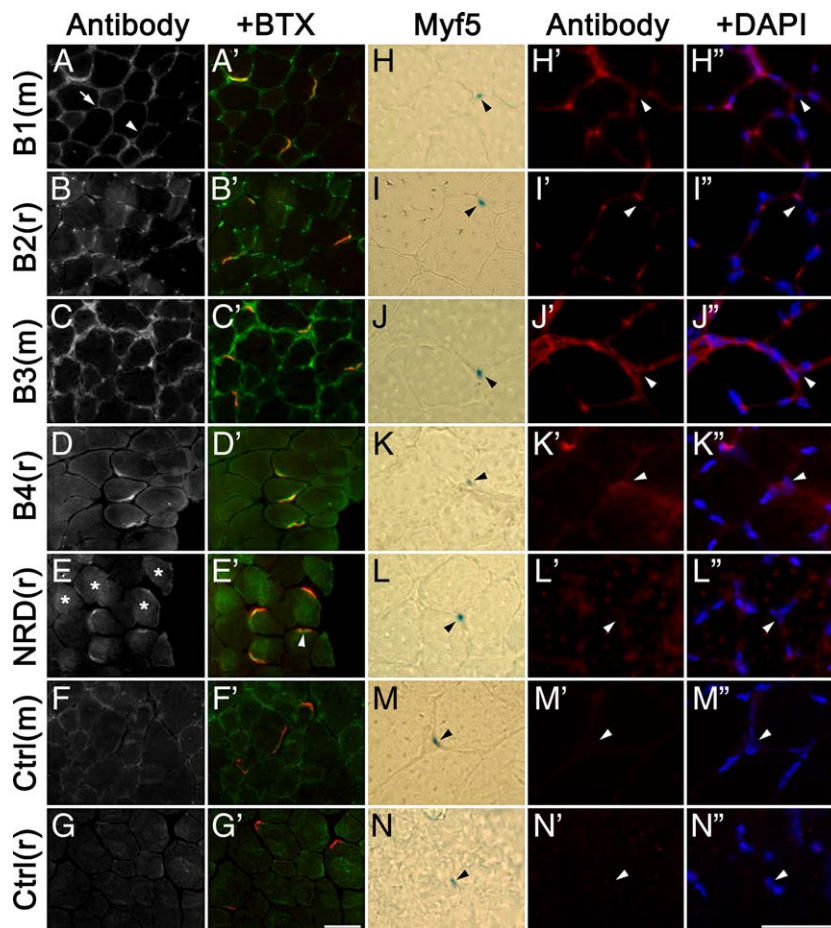


**Fig. 1 – ErbB receptor distribution on undamaged panel muscles.** (A–G') C57Bl/10 TA muscle transverse sections were dual stained with receptor-specific antibodies (green in merged images) and  $\alpha$ -bungarotoxin to label the NMJ (BTX, red in merged images). Host species of primary antibody is denoted by mouse (m) or rabbit (r) in parenthesis after the antibody name. ErbB1 is present on myofibre surfaces (arrowhead in panel A) and on interstitial tissues and capillaries (arrow in A). (E, E') NRDC is occasionally present deep to the NMJ (arrowhead in panel E') and identifies a subset of myofibres (asterisks in E). (H–N'')  $Myf5^{nLacZ/+}$  TA muscle transverse sections, triple labelled with (H–N) X-gal to identify  $Myf5+$  satellite cell nuclei; (H'–L') receptor-specific antibodies; and (H''–N'') merged antibody and DAPI nuclear stain images. Satellite cell nuclei are marked with an arrowhead in each series of images. (F, M') Ctrl(m) and (G, N') Ctrl(r) are, respectively, mouse and rabbit IgG controls photographed under identical conditions. Scale bars are 50  $\mu$ m. (For interpretation of the references to colour in this figure legend, the reader is referred to the web version of this article.)

## 282 Localisation of *erbB* receptors during activation of satellite cells

283 Isolated EDL myofibre preparations, free of connective tissue,  
 284 capillaries and other non-muscle cells were maintained in  
 285 10% serum-containing medium for between 6 and 48 h.  
 286 During this period, the satellite cells associated with each  
 287 myofibre become activated (by the criterion of *MyoD* expres-  
 288 sion) and at around 24 h enter into vigorous cell division with  
 289 a resultant rapid amplification of their myogenic progeny  
 290 [4,42].

291 During the earliest stages of activation from quiescence  
 292 (within the first 6 h), neither *MyoD* immunoreactivity nor *Myf5*  
 293 expression accurately identify all satellite cells [4,42]. There-  
 294 fore, to investigate *erbB* receptor distribution on satellite cells  
 295 at 6 h in vitro (T6), we used EDL myofibres isolated from the  
 296 MLC-3F<sup>nLacZ</sup> transgenic mouse, in which  $\beta$ -galactosidase is  
 297 expressed exclusively by differentiated myonuclei. This

approach allows the identification of all of the associated 298  
 satellite cells, as they do not express the transgene and 299  
 therefore fail to stain with X-gal [42] (Figs. 2A–G'). Note that in 300  
 those cells expressing  $\beta$ -galactosidase the intensely coloured 301  
 X-gal reaction product masks the underlying DAPI nuclear 302  
 fluorescence.) Typically, about 8 satellite cells are associated 303  
 with each EDL myofibre [4]. At T6, *erbB1* was detectable on  $1.8 \pm$  304  
 $0.4$  satellite cells per myofibre; about one quarter of the satellite 305  
 cell population ( $23/92$  of the X-gal-negative cells on 13 fibres  $\pm$  306  
 SEM, Figs. 2A–A''). *erbB2* was detectable on all satellite cells, 307  
 with  $4.4 \pm 0.5$  satellite cells per myofibre (about half the 308  
 population) being strongly immunofluorescent ( $84/165$  of the 309  
 X-gal-negative cells on 19 fibres  $\pm$  SEM; strongly *erbB2* immu- 310  
 nofluorescent cell arrowed; Fig. 2B''). *erbB3* was only weakly 311  
 detected and was present on  $1.4 \pm 0.4$  satellite cells per 312  
 myofibre; about 15% of the population ( $20/132$  of the X-gal- 313  
 negative cells on 14 fibres  $\pm$  SEM, Fig. 2C). By contrast, *erbB4* 314

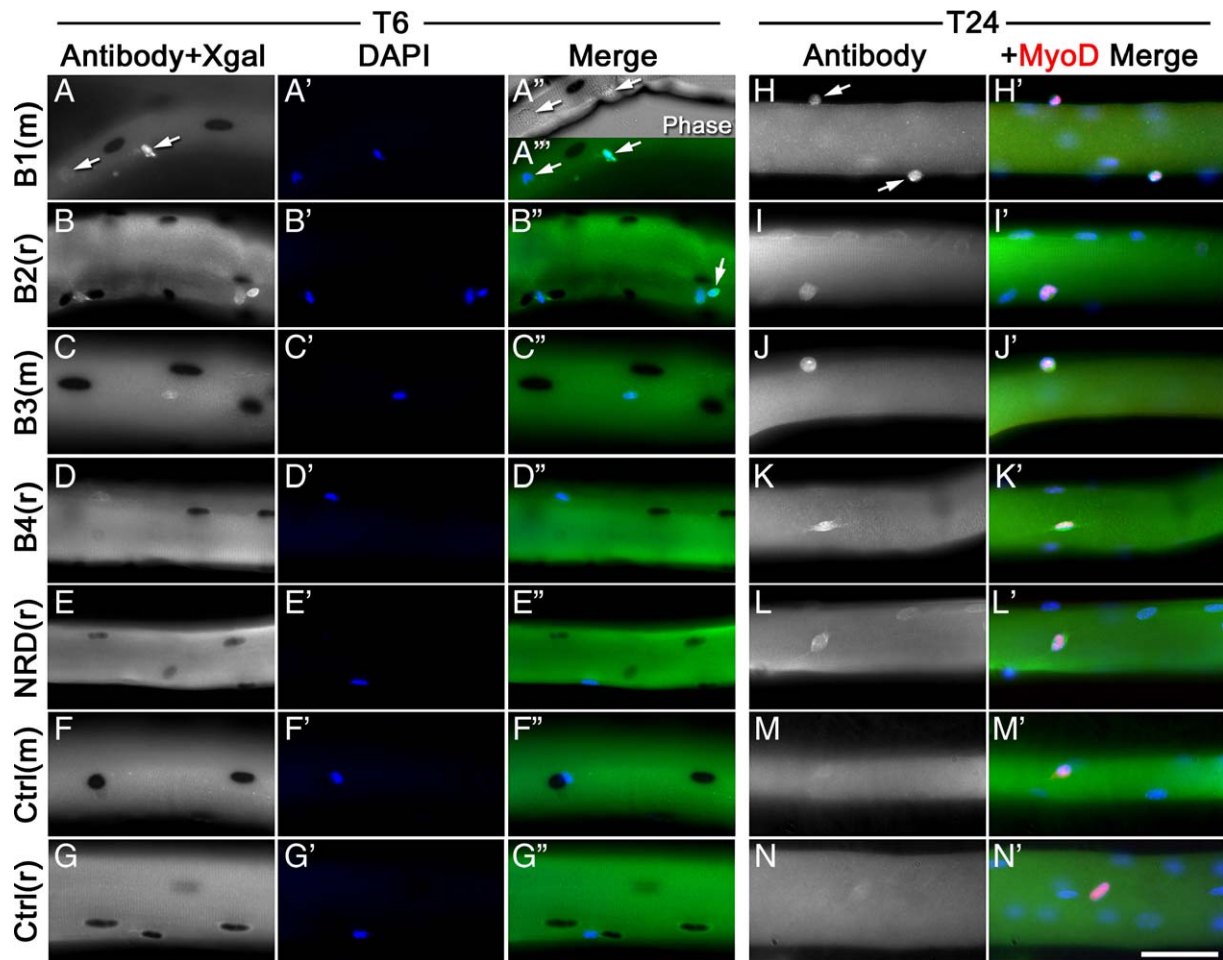


**Fig. 2** – Following injury, erbB receptors become localised to activating satellite cells. Isolated EDL myofibres immunostained with receptor-specific antibodies (green in merged images) and DAPI (blue) following 6 or 24 h in 10% serum-containing medium. Host species of primary antibody is denoted by mouse (m) or rabbit (r) in parenthesis after the antibody name. (A–G'') 6 h: MLC-3F<sup>nLacZ</sup> transgenic myofibres, in which myonuclei stain darkly with X-gal. (A–A'') Approximately 25% of satellite cells show erbB1 immunoreactivity (compare the two arrowed satellite cells). (B–B'') All satellite cells are erbB2 immunopositive, with about half showing strong immunoreactivity (arrowed in B''). (H–H') 24 h: Myofibres from C57Bl/10 mice. MyoD is red in merged images. (H–H') ErbB1 immunoreactivity showed variations within the satellite cell population (compare the two cells arrowed in H). (F, M) Ctrl(m) and (G, N) Ctrl(r) are, respectively, mouse and rabbit IgG controls photographed under identical conditions. Scale bar is 50  $\mu$ m. (For interpretation of the references to colour in this figure legend, the reader is referred to the web version of this article.)

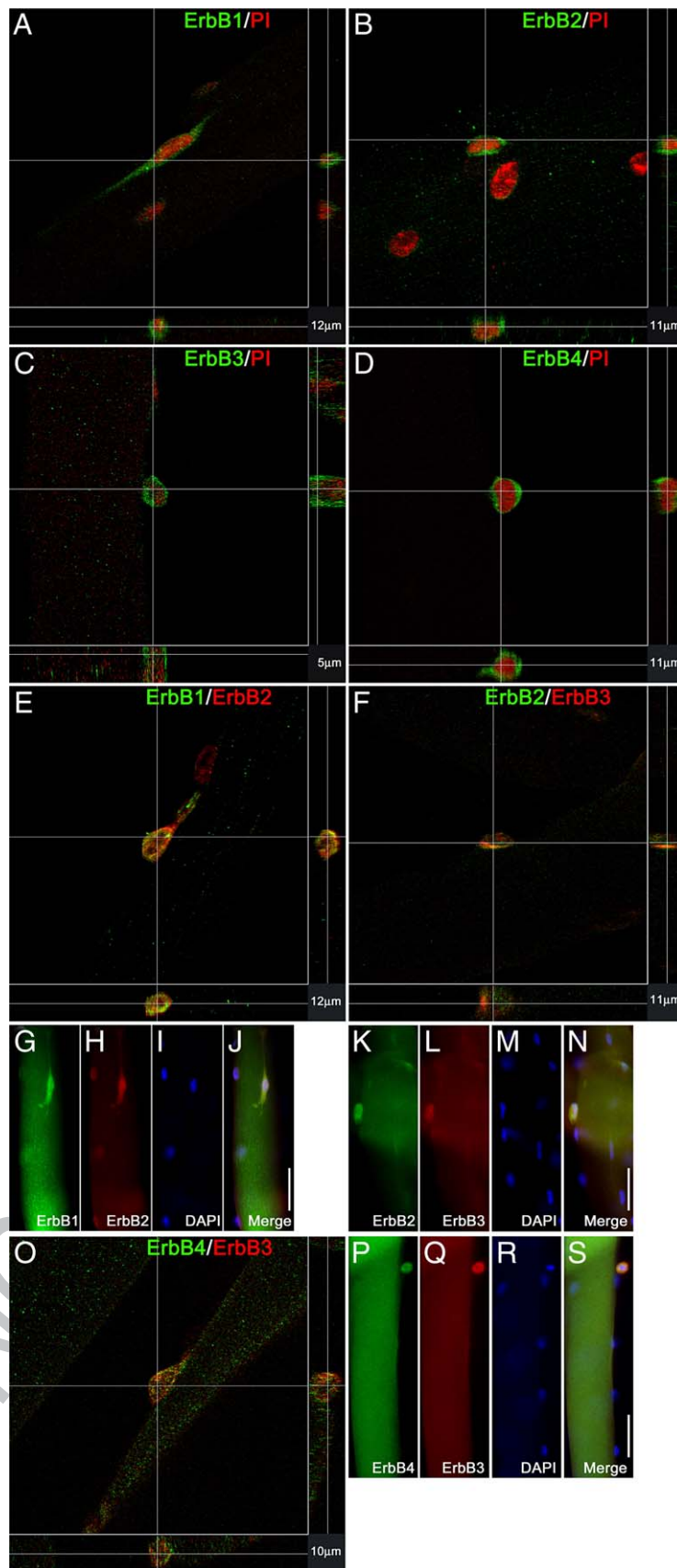
315 (Fig. 2D) and NRDC (Fig. 2E) were not detected (compare with  
316 serum controls in Figs. 2F, G).

317 After 24 h in vitro, virtually all myofibre-associated satellite  
318 cells can be identified by the expression of MyoD [4]. Thus, for  
319 experiments at 24 h and later we used EDL myofibres isolated  
320 from C57Bl/10 mice, dual stained with MyoD and erbB  
321 receptor-specific antibodies.

322 After 24 h in vitro (T24), erbB1 was detectable on all MyoD+  
323 satellite cells, with intense immunofluorescence observed on  
324  $2.9 \pm 0.5$  satellite cells per myofibre (41/82 MyoD+ cells on 14  
325 fibres  $\pm$  SEM, compare the intensities of the two satellite cells  
326 arrowed in Fig. 2H). All other receptor antibodies demon-  
327 strated a uniformity of robust immunofluorescence labelling  
328 throughout the MyoD+ satellite cell population. Some MyoD-  
329 myonuclei demonstrated weak immunoreactivity with anti-  
330 NRDC at T24 (Fig. 2L). Confocal microscopy of T24 myofibres,

331 dual stained with individual anti-erbB antibodies and the  
332 nuclear marker propidium iodide, confirmed the surface/  
333 cytoplasmic location of erbB1-4 (Figs. 3A–D). Moreover, both  
334 confocal microscopy (Figs. 3E, F, O) and conventional epifluo-  
335 rescence microscopy (Figs. 3G–J, K–N, P–S) revealed co-localisa-  
336 tion of erbB1/erbB2, erbB2/erbB3 and erbB3/erbB4 in activated  
337 satellite cells.

338 After 48 h in vitro (T48), all myoblasts on isolated mouse  
339 EDL myofibres had become strongly immunoreactive for  
340 erbB1, erbB2, erbB4 and NRDC, while erbB3 was now only  
341 weakly detected (Figs. 4A–E'). After 48 h, myoblasts on isolated  
342 myofibres diversify with respect to MyoD expression: a  
343 minority reduce their levels of MyoD and return to an  
344 undifferentiated quiescent state, while the majority maintain  
345 MyoD and eventually express myogenin as they enter  
346 terminal differentiation [10]. Importantly, we found that the



347 immunofluorescence intensity of erbB receptor and NRDC  
 348 staining on satellite cells at T48 was equivalent across the  
 349 entire population, irrespective of variations in MyoD immu-

noreactivity (in Figs. 4C", H', I' myoblasts showing reduced 350  
 MyoD staining are marked with arrowheads). However, by T72, 351  
 the immunofluorescence intensity of erbB2 on isolated EDL 352

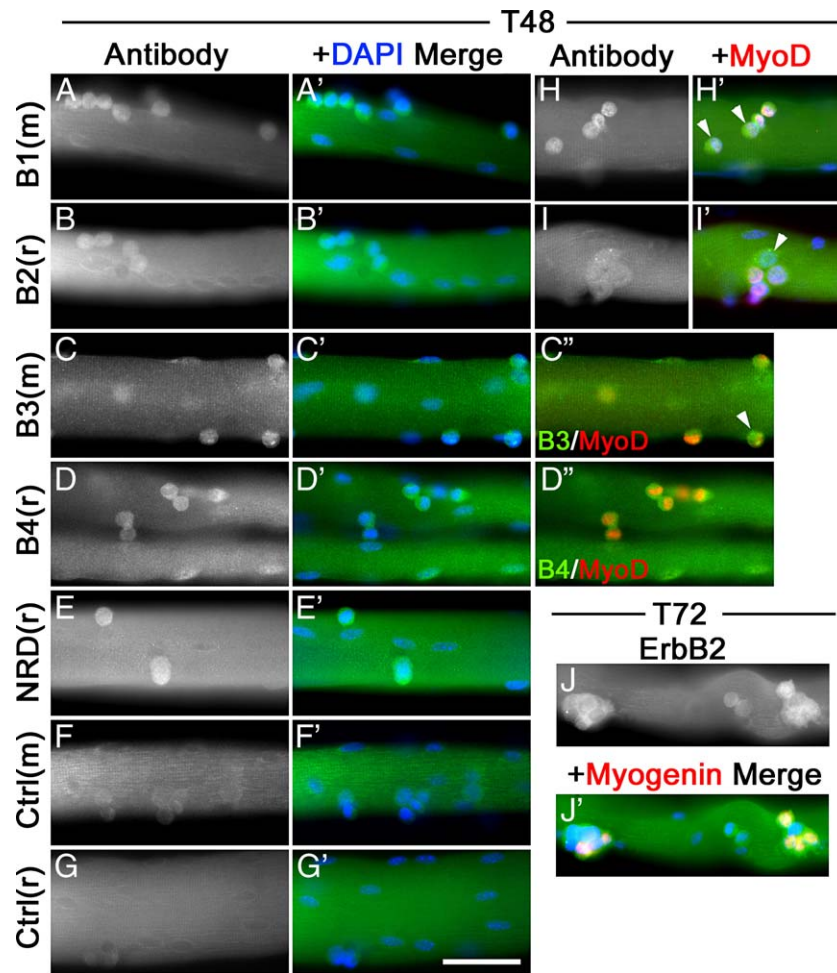


**Fig. 4** – Isolated EDL myofibres immunostained following (A–I') 48 h or (J–J') 72 h in 10% serum-containing medium with receptor-specific antibodies (green in merged images). Host species of primary antibody is denoted by mouse (m) or rabbit (r) in parenthesis after the antibody name. Arrowheads in (H', I' and C') show a subpopulation of myoblasts labelled with receptor antibodies even when MyoD (red in merged images) is down-regulated. (J–J') 72 h: ErbB2 immunoreactivity in green and myogenin immunoreactivity in red. (F) Ctrl(m) and (G) Ctrl(r) are, respectively, mouse and rabbit IgG controls photographed under identical conditions. Scale bar is 50  $\mu\text{m}$ . (For interpretation of the references to colour in this figure legend, the reader is referred to the web version of this article.)

353 myofibres did exhibit variation within the myoblast popula- 364  
 354 tion (Fig. 4), being more intense on cells that had committed 365  
 355 to differentiation and were co-expressing myogenin (Fig. 4J').

### 356 Not all satellite cells have active *erbB* receptors

357 To begin to address what functions *erbB* receptors might play 368  
 358 during satellite cell activation, we first determined if the 369  
 359 receptors are functional. *ErbB* ligand growth factors are 370  
 360 present in normal serum [43–45] and should therefore be 371  
 361 freely available in our culture medium. EDL myofibre prepara- 372  
 362 tions were maintained in vitro for 24 h and then immunos- 373  
 363 tained with antibodies specific to phosphorylated (active) 374

forms of *erbB1* and *erbB2*. On average,  $4.5 \pm 1.1$  cells per 364  
 myofibre ( $n=11$  fibres) were immunopositive for phospho- 365  
 rylated *erbB1* (Figs. 5A, B) and  $2.7 \pm 0.5$  cells per fibre ( $n=10$  fibres) 366  
 were immunopositive for phosphorylated *erbB2* (Figs. 5E, F). 367  
 The average number of satellite cells on each of these 368  
 myofibres was determined to be  $6.8 \pm 0.5$  by subsequent Pax7 369  
 immunostaining (not shown). As expected, when T24 cultured 370  
 myofibres were treated with alkaline phosphatase, prior to 371  
 immunostaining with anti-phosphorylated *erbBs*, no immu- 372  
 nopositive cells were detected (*erbB1* control, Figs. 5C, D; *erbB2* 373  
 control, Figs. 5G, H), confirming that these antibodies recog- 374  
 nise only the phosphorylated forms of the receptors. Because 375  
*erbB1* and *erbB2* receptors are exclusively detected on all 376

**Fig. 3** – (A–D) Confocal images of C57Bl/10 isolated EDL myofibres after 24 h in 10% serum containing medium, immunostained with *erbB* receptor-specific antibodies (green channel) and propidium iodide nuclear marker (PI, red channel). (E, F, O) Co-expression of *erbB* receptors on satellite cells at T24. Each confocal image is a field  $100 \mu\text{m} \times 100 \mu\text{m}$  square. The z-axis depth of each confocal image is marked in the bottom right corner. (G–N, P–S) Corresponding epifluorescence images of double immunostained myofibres, plus DAPI nuclear stain. Scale bars in epifluorescence images are 50  $\mu\text{m}$ .

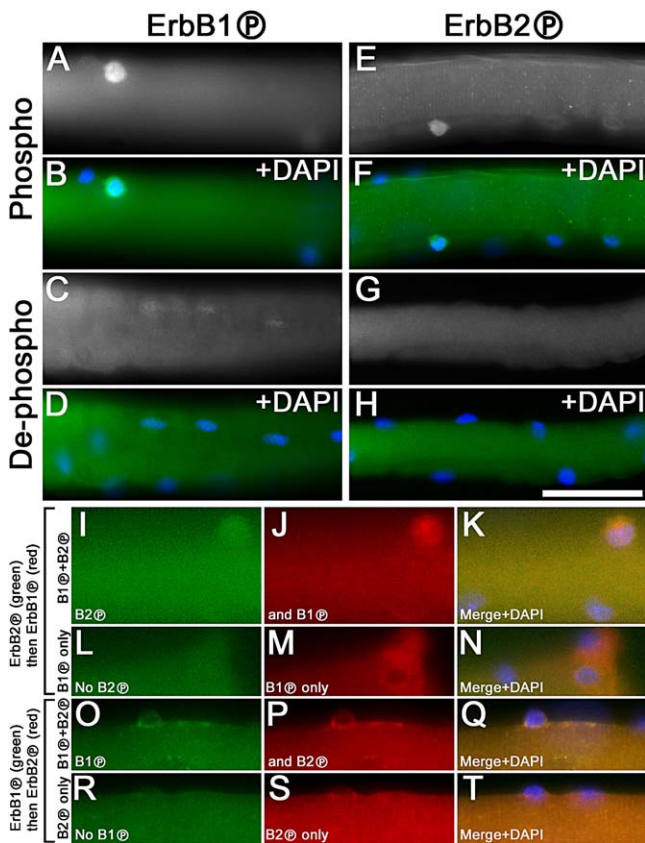


**Fig. 5 – (A–H)** EDL isolated myofibres cultured for 24 h and immunostained with antibodies specific to (A–D) phosphorylated erbB1 and (E–H) phosphorylated erbB2. (C, D, G, H) Myofibres pre-treated with alkaline phosphatase confirmed the specificity of the antibodies for the phosphorylated forms of the receptors. (I–T) Sequential immunostaining with the anti-phospho antibodies identified cells that contained a mixture of phosphorylated erbB1 and phosphorylated erbB2 (I–K and O–Q), but also cells that had exclusively either (M) phosphorylated erbB1 or (S) phosphorylated erbB2. DAPI counterstaining (blue) identifies cell nuclei. “p” = phosphorylated. Scale bar is 50  $\mu\text{m}$ . (For interpretation of the references to colour in this figure legend, the reader is referred to the web version of this article.)

377 satellite cells by T24 (Fig. 2), this implies that at any one time  
 378 only about 66% of satellite cells are stimulated via erbB1 and  
 379 39% via erbB2 signalling pathways. No pattern was detected in  
 380 the distribution of these “stimulated” satellite cells along  
 381 myofibres. In order to help determine whether erbB1 and  
 382 erbB2 are active in the same cells, we sequentially immunos-  
 383 tained T24 myofibres with anti-phospho erbB1 then Alexa 488  
 384 secondary antibody, followed by anti-phospho erbB2 then  
 385 Alexa 594 secondary antibody. Some T24 myofibres were  
 386 stained in the opposite sequence, i.e., anti-phospho erbB2 was  
 387 applied first (Figs. 5I–T). We found that 12.9% of labelled cells  
 388 (4/31 cells on 9 myofibres) labelled exclusively with anti-  
 389 phospho erbB1 when this was the final layer (compare Figs. 5L  
 390 and M), while 3.2% of labelled cells (2/63 cells on 16 myofibres)  
 391 were exclusively anti-phospho erbB2 immunopositive when  
 392 this was the final layer (compare Figs. 5R and S). Thus, the

remaining 83.9% of anti-phospho erbB immunostained cells  
 contain both erbB1 and erbB2 in their phosphorylated forms,  
 corresponding to about three cells per fibre in this experiment.

*ErbB ligand growth factors prevent early myoblast cell death* 396

To investigate the consequences of erbB ligand withdrawal,  
 EDL-isolated myofibre preparations were maintained in 10%  
 serum-containing medium for 24 h, to allow up-regulation of  
 erbB receptors on the satellite cells. At this point, the  
 preparations were separated into different culture conditions  
 for a further 24 h (between T24 and T48). Some continued to be  
 maintained in 10% serum medium, while others were washed  
 in DMEM and transferred into serum-free DMEM and supple-  
 mented with either: nothing, 1 nM EGF (erbB1 ligand), 1 nM HB-  
 EGF (erbB1,4 and NRDC ligand), 1 nM neuregulin (NRG) (erbB3,4  
 ligand) or a 1-nM mixture of all three erbB ligand growth  
 factors. Immunostaining confirmed that all erbB receptors and  
 NRDC were still present on myoblasts in preparations deprived  
 of serum between T24 and T48, although the immunofluores-  
 cence intensity for erbB1 was reduced (not shown).

As expected, there was a significant difference ( $P < 0.001$ )  
 between the numbers of Pax7+ cells per fibre when comparing  
 serum-maintained with unsupplemented serum-free condi-  
 tions (compare Figs. 6A and D). Importantly, however, this  
 was not simply attributable to differences in proliferation,  
 since the numbers of Pax7+ cells associated with serum-de-  
 prived myofibres was significantly below ( $P < 0.01$ ) their start-  
 ing value on T0 myofibres (Fig. 6G). Supplementation with  
 1 nM NRG or 1 nM EGF alone similarly resulted in a significant  
 loss of Pax7+ cells compared to T0 ( $P < 0.01$  and  $P < 0.001$ , res-  
 pectively; Fig. 6G). By contrast, supplementing serum-free  
 medium with 1 nM HB-EGF or a 1-nM mixture of all three  
 growth factors prevented the loss of Pax7+ cells compared  
 with T0 (Fig. 6G).

A similar trend was seen with MyoD immunoreactivity.  
 Thus, serum-deprived myofibres were associated with sig-  
 nificantly fewer MyoD+ cells than serum-maintained controls  
 ( $P < 0.001$ ; compare Figs. 6B and E). Supplementing serum-free  
 cultures with a 1-nM mixture of growth factors resulted in a  
 significant increase in the number of MyoD+ cells per fibre  
 compared to serum-free controls ( $P < 0.001$ ; Fig. 6G). However,  
 serum-free cultures supplemented with 1 nM NRG or 1 nM EGF  
 had significantly fewer MyoD+ cells per myofibre than  
 cultures supplemented with the growth factor mixture  
 ( $P < 0.001$  and  $P < 0.01$ , respectively, in Fig. 6G). The number of  
 MyoD+ cells per fibre was statistically indistinguishable  
 between growth factor mixture-supplemented and HB-EGF-  
 supplemented myofibres (Fig. 6G). Although the growth factor  
 mixture increased the number of MyoD+ cells compared to  
 DMEM, or NRG or EGF, it was not as efficient as 10% serum  
 in generating large numbers of MyoD+ cells ( $P < 0.05$ ; Fig. 6G).

To assess the role of erbB3 activity in promoting satellite cell  
 survival, a function-blocking concentration of anti-erbB3 anti-  
 body (10  $\mu\text{g}/\text{ml}$  [46]) was added to serum-maintained myofibre  
 cultures between T24 and T48. Anti-erbB3 had no effect on the  
 numbers of Caspase8+ cells per myofibre (control:  $4.25 \pm 0.7$ ,  
 $n = 12$  myofibres; anti-erbB3:  $4.29 \pm 0.6$ ,  $n = 14$  myofibres) but  
 did significantly ( $P = 0.013$ ) reduce the number of MyoD+ cells  
 per myofibre from  $14.1 \pm 1.0$  ( $n = 15$  myofibres) to  $10.0 \pm 1.2$

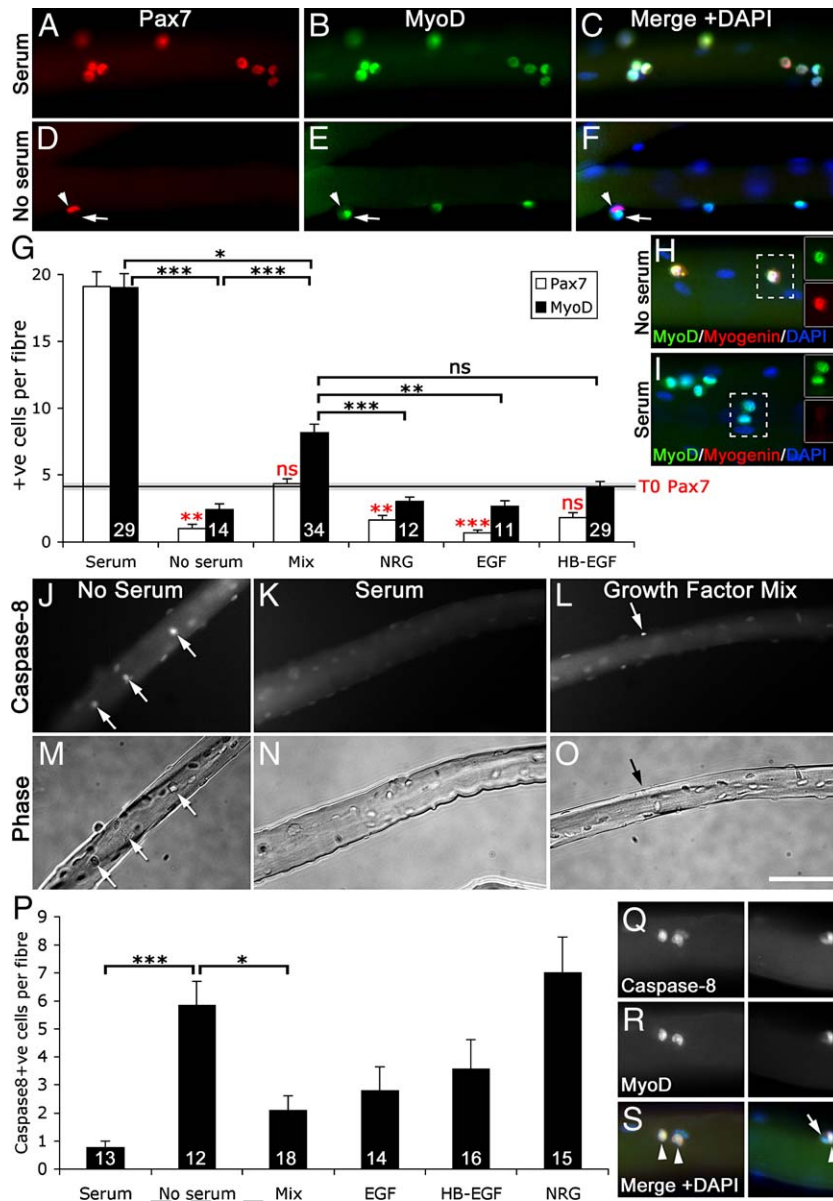


**Fig. 6 – ErbB ligand growth factors protect myoblasts from apoptosis.** (A–F) Myofibres were maintained in the absence of serum between T24 and T48 and stained for Pax7 (red), MyoD (green) and DAPI (blue). Some cells are returning to quiescence (Pax7+/MyoD– cell identified with arrowhead) and others are differentiating (Pax7–/MyoD+ cell identified with arrow). (G) Comparisons of the mean numbers of Pax7+ and MyoD+ cells per myofibre, on myofibres maintained either in serum, or in serum-free conditions (with or without individual growth factors or a mixture of growth factors). T0 Pax7 indicates the mean number of Pax7+ cells on T0 myofibres. (H, I) Expression of myogenin (red) and MyoD (green) in serum-containing and in serum-free conditions. The fluorescence channels corresponding to the boxed regions in the merged images are shown as separate insets. (J) Many cells activated caspase-8 in serum-free conditions (arrows). (L) Caspase-8 activation was substantially prevented by the mixture of growth factors (arrows), quantified in panel P. (M–O) corresponding phase contrast images. (Q–S) The majority of apoptotic cells were MyoD+ (arrowheads in merged image S). A rare caspase8+/MyoD– exception is arrowed in panel S (inset). DAPI counterstaining (blue) identifies cell nuclei. Scale bar is 100  $\mu$ m for panels J–O. For all other images, this bar is 50  $\mu$ m. Statistical analyses: \* $P < 0.05$ , \*\* $P < 0.01$ , \*\*\* $P < 0.001$ , ns = not significant. (For interpretation of the references to colour in this figure legend, the reader is referred to the web version of this article.)

451 (n = 18 myofibres). Any effects of anti-erbB3 on cell proliferation  
452 were not assessed.

453 As myoblasts withdraw from the cell cycle as a prelude to  
454 terminal differentiation, they begin to express myogenin and  
455 subsequently down-regulate MyoD. However, differentiation

cannot account for the lower numbers of MyoD+ cells upon 456  
serum withdrawal. Differentiation was apparent in the pre- 457  
parations maintained from T24 to T48 in serum-free condi- 458  
tions, since 94.4% (51/54) of MyoD+ cells co-expressed 459  
myogenin (Fig. 6H). In contrast, no myogenin+ cells (0/162) 460

were present on myofibres maintained in 10% serum (Fig. 6I). Growth factor supplementation had no effect on the proportion of differentiating cells compared to serum-deprived myofibres (1 nM EGF: 92.1% (82 myogenin+/89 MyoD+); 1 nM HB-EGF: 89.8% (53/59); 1 nM NRG: 95.7% (44/46); or a 1-nM growth factor mixture: 97.2% (69/71)). Crucially, no MyoD-/myogenin+ cells were detected on serum-deprived myofibres. This is important because it shows that upon serum deprivation, all the differentiating myogenin+ cells continue to express MyoD. Therefore, the observed reduction in the number of MyoD+ cells must indeed represent a true absence of these cells and not simply a differentiation-induced change of phenotype. An alternative explanation for the loss of MyoD+ cells might be that serum-deprived myoblasts return to their Pax7+/MyoD-quiescent state. However, since the number of Pax7+ cells is also reduced, to significantly less than the T0 value, a return to quiescence can be discounted.

To determine whether apoptotic cell death might account for the loss of MyoD+ cells upon serum deprivation, we assayed myofibre preparations for the activation of caspase-8. Caspase-8 was chosen because it is activated very early during apoptosis, being a critical initiator of the death receptor pathway [47], but additionally regulating the mitochondrial pathway by promoting the activation of Bax and Bak [48]. Furthermore, caspase-8 is activated by singlet oxygen ROS, upstream of caspase-3 activation [49]. In the absence of serum between T24 and T48, six-fold more cells on myofibres activated caspase-8 than in serum-containing control conditions (compare Figs. 6J, M with Figs. 6K, N; quantified in Fig. 6P). The majority of apoptosing caspase-8+ cells on T24-T48 serum-deprived myofibres were also MyoD+ (73.7%, 14/19 cells; Fig. 6S). Conversely, and in agreement with the Pax7/MyoD immunoreactivity data of Fig. 6G, serum-deprived myofibre preparations supplemented with a 1-nM mixture of growth factors demonstrated significantly less caspase-8 activation than serum-deprived controls ( $P < 0.05$ ; Figs. 6L, O, P). Serum-deprived preparations supplemented with 1 nM EGF or 1 nM HB-EGF, but not 1 nM NRG alone, also demonstrated reduced caspase-8 activation (Fig. 6P). Although it is clear that apoptosis is initiated in MyoD+ myoblasts in response to serum deprivation (Figs. 6J-S), because caspase-8 activity was only assayed at T48, we cannot formally conclude that apoptosis is the only mechanism by which myoblasts are lost during the T24-T48 period of serum deprivation.

Taken together, these data suggest that a mixture of erbB1/erbB4 ligands (EGF and HB-EGF) but not an erbB3/erbB4 ligand (NRG) act to protect activated satellite cells and their myoblast progeny from cell death.

#### 509 Inhibition of erbB2 signalling promotes myoblast apoptosis

ErbB1 is the common receptor bound by EGF and HB-EGF, although subsequent signal transduction can occur either via erbB1 homodimers or via erbB1/erbB2 heterodimers [50,51]. To determine whether inhibition of either erbB1 or erbB2 signalling leads to satellite cell or myoblast apoptosis, we examined caspase-8 activity in myofibre preparations cultured for 6 h, 24 h or 48 h in 10% serum-containing medium supplemented with highly specific inhibitors of erbB1 or erbB2 tyrosine phosphorylation: AG1478 and AG825, respectively [37] (Figs.

7A-N). By T24, approximately two times more cells exhibited caspase-8 activity in the presence of AG825 (Figs. 7E, M) compared to either AG1478 (Fig. 7G, M) or unsupplemented controls (Figs. 7H, M). These preparations were subsequently immunostained, revealing that it was predominantly Pax7+ satellite cells that were undergoing apoptosis (arrowheads in Figs. 7B', F', J'). Although AG825-induced caspase-8 activation peaked at T24 (Fig. 7M), it took a further 24 h for this initiation of cell death to be reflected in a significant depletion of Pax7+ cells on AG825-treated myofibres (Fig. 7N). Thus, AG825 resulted on average in a loss of one Pax7+ cell per fibre (~15% of the satellite cell population) by T24, and four Pax7+ cells per fibre by T48, compared to unsupplemented controls (Fig. 7N). The erbB inhibitors did not affect satellite cell activation or cell cycle progression. Thus, in separate experiments, Pax7+ satellite cells activated MyoD as normal in the presence of AG825 (T0-T24 AG825: 189 Pax7+/184 MyoD+,  $n=26$  fibres. T0-T24 control: 284 Pax7+/277 MyoD+,  $n=30$  fibres); while 95 of 96 Pax7+ cells incorporated BrdU (from 9 fibres) during 48 h in the continuous presence of AG825 plus BrdU.

The loss of Pax7+ cells in the presence of AG825 appeared modest, although consistent with the values obtained from the serum-free growth factor supplementation experiments (Fig. 6G). To better model the oxidative stresses that myofibres are subjected to immediately following damage in vivo, we maintained myofibres in 10% serum-containing medium for 6 h to allow erbB receptors to become up-regulated (see Fig. 2), and then supplemented half of the myofibre preparations with 100  $\mu$ M hydrogen peroxide ( $H_2O_2$ ), with or without erbB inhibitors, for a further 18 h until T24. This concentration of  $H_2O_2$  was chosen because it is high enough to induce a stress response in myofibres but does not affect their viability [52]. The presence of  $H_2O_2$  in itself did not cause a significant loss of Pax7+ cells (Fig. 7O). Only in cultures co-supplemented with  $H_2O_2$  and AG825 or AG1478 were there significant losses of Pax7+ cells (Fig. 7O).

TUNEL provides a sensitive indicator of late-stage apoptotic cells, after DNA fragmentation has occurred. Consistent with the caspase-8 results, exposure of myofibres to AG825 in 10% serum-containing medium for 24 h led to an increase in the proportion of dual TUNEL+/Pax7+ cells per fibre ( $10.7 \pm 4.4\%$ ,  $n=10$  fibres; Figs. 7P-R), compared to unsupplemented controls ( $4.6 \pm 2.1\%$ ,  $n=18$  fibres; Figs. 7S-U).

#### Pro- and anti-apoptotic signals in activating satellite cells

Signal transduction via erbB receptors can activate several distinct intracellular signalling pathways that include phosphatidylinositol 3' kinase/protein kinase B (PI3-K/Akt), Ras/mitogen-activated protein kinase (Ras/MAP-K) and phospholipase C $\gamma$ /protein kinase C (PLC $\gamma$ /PKC) [22,24]. In addition, erbB2 (via erbB1-erbB2 heterodimers) directly phosphorylates the transcription factor STAT3 [53]. Each of these erbB signal transduction pathways has been implicated in opposing survival and apoptosis decisions within a variety of cell-types, including muscle [54-57]. Therefore, in order to identify the pro-and anti-apoptotic signalling pathways operating in satellite cells during the first 24 h in culture, we examined the effects of inhibitors specific to these various pathways.

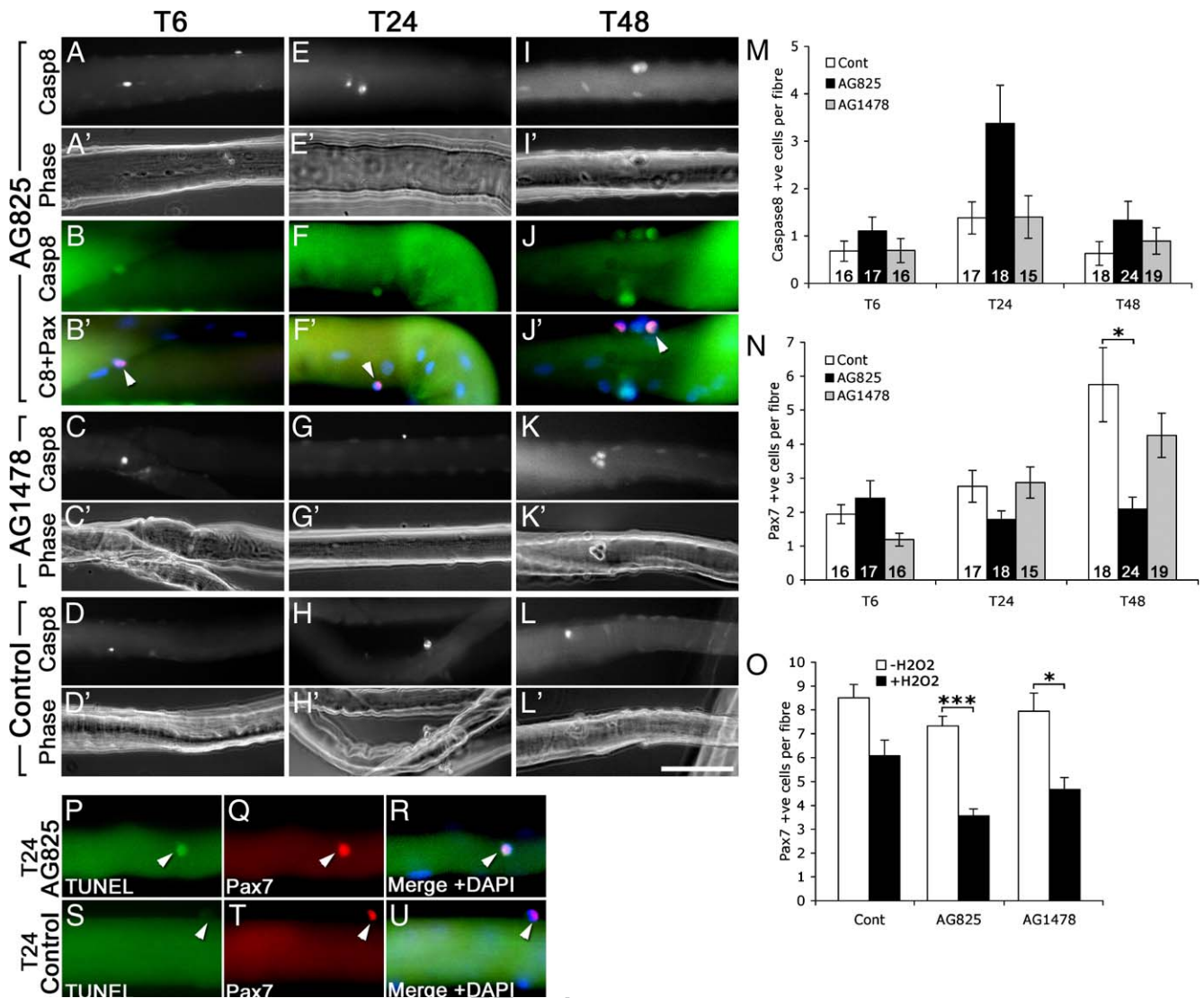


**Fig. 7** – Inhibition of erbB2 function leads to satellite cell and myoblast apoptosis. (A–L') Mouse isolated EDL myofibres show similar levels of caspase-8 activation following 6 h or 48 h exposure to AG825, AG1478 or control conditions. (E–H') Following 24 h exposure many more cells demonstrate caspase-8 activation in (E) AG825, than in (G) AG1478, or (H) control conditions. (B', F', J') Double caspase-8/Pax7 immunostaining reveals that satellite cells are the predominant apoptosing cell type at each time point (double-positive cells marked with arrowheads). (M) Graphical representation of the caspase-8 data, illustrating the peak of AG825-induced apoptosis at T24. (N) Number of Pax7+ cells per myofibre in the presence of AG825 or AG1478, compared to control. (O) Between T0 and T24, AG825 and AG1478 cause significant losses of Pax7+ satellite cells under conditions of elevated oxidative stress (supplementation with 100  $\mu$ M H<sub>2</sub>O<sub>2</sub>). (P–U) Double TUNEL/Pax7 immunostaining confirmed satellite cell apoptosis following 24 h exposure to AG825 (P–R), but not in control conditions (S–U). Statistical analyses: \* $P < 0.05$ , \*\*\* $P < 0.001$ .

577 EDL myofibres, isolated from the same mouse, were  
 578 maintained for 24 h in 10% serum-containing medium in the  
 579 continuous presence of individual inhibitors, with or without  
 580 AG825, and were then assayed for caspase-8 activity, followed  
 581 by dual Pax7/MyoD immunostaining. The numbers of immu-  
 582 nopositive and caspase-8+ cells were counted on 15–20  
 583 myofibres per condition (Fig. 8A). This batch of myofibres  
 584 had more satellite cells per fibre and was twice as sensitive to  
 585 AG825 than the group used in Figs. 7A–N; with four-fold more  
 586 caspase-8+ cells per fibre and an average loss of two Pax7+  
 587 satellite cells per fibre following 24 h in AG825, compared with  
 588 untreated control myofibres (Fig. 8A).

Inhibition of STAT3 resulted in a similar level of caspase-8 589  
 activation to that seen following erbB2 inhibition. However, 590  
 despite this high caspase-8 activity, satellite cell numbers 591  
 were reduced by on average only one satellite cell per 592  
 myofibre. Co-inhibition of STAT3 and erbB2 caused hypercon- 593  
 traction of all fibres, precluding further analysis. These data 594  
 indicate an anti-apoptotic role for the STAT3 pathway during 595  
 satellite cell activation from quiescence (Fig. 8A). 596

Inhibition of Akt resulted in an average loss of one satellite 597  
 cell per fibre, although caspase-8 was not elevated; suggesting 598  
 a slight protective, although not necessarily anti-apoptotic, 599  
 role for Akt signalling (Fig. 8A). 600

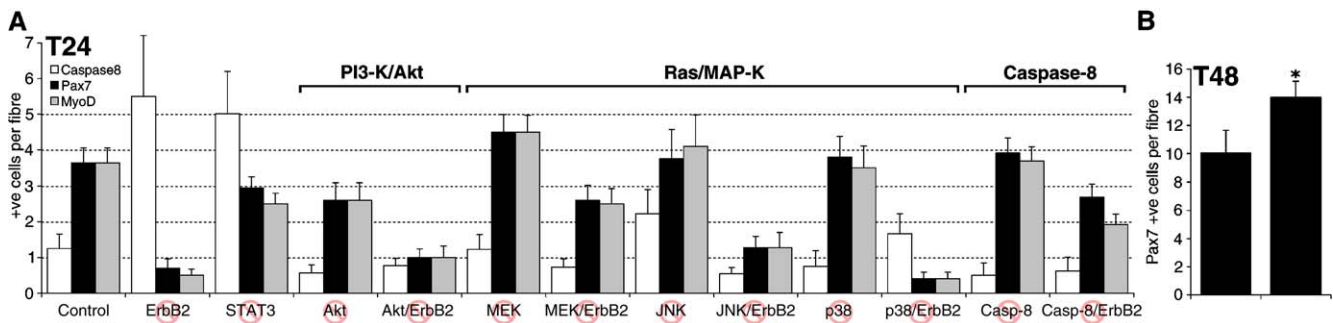


**Fig. 8 – (A) Myofibres were exposed to a variety of signal transduction pathway inhibitors for 24 h, in the absence or presence of the erbB2 inhibitor AG825 (inhibited pathways indicated on x-axis). The number of caspase-8+, Pax7+ and MyoD+ cells per myofibre were quantified for each condition. (B) Effect of transient inhibition of MEK (between T0 and T24) on the numbers of Pax7+ cells per myofibre at T48. Statistical analyses: \* $P < 0.05$ .**

601 Conversely, inhibition of MEK resulted in a net gain of one  
 602 satellite cell per fibre compared with controls. Importantly, all  
 603 satellite cells counted following MEK inhibition were well-  
 604 isolated singlets, with no evidence of premature cell division  
 605 compared with the control preparations. Moreover, co-inhibition  
 606 of MEK and erbB2 partially rescued the loss of satellite cells  
 607 seen with erbB2 inhibition alone. This would suggest that the  
 608 Ras/MEK pathway has a net pro-apoptotic effect during  
 609 satellite cell activation, accounting for a background loss of  
 610 one satellite cell per fibre by T24 under our relatively benign  
 611 10% serum-containing medium culture conditions (Fig. 8A).

612 Inhibition of JNK or p38 MAP-K pathways had no effect on  
 613 satellite cell numbers, even though JNK inhibition caused a  
 614 slight increase in caspase-8 activation (Fig. 8A). Inhibition of  
 615 PLC $\gamma$ /PKC caused myofibre hypercontraction within 24 h, pre-  
 616 venting any analysis of satellite cells under these conditions.

617 The control number of satellite cells per fibre was main-  
 618 tained following competitive inhibition of caspase-8. Dual  
 619 caspase-8/erbB2 co-inhibition partially prevented the loss of  
 620 satellite cells seen following erbB2 inhibition alone ( $2.7 \pm 0.4$   
 621 versus  $0.7 \pm 0.3$  Pax7+ cells per fibre,  $n = 16$  fibres), confirming  
 622 that satellite cell death following erbB2 inhibition occurs via  
 623 caspase-8-mediated apoptosis (Fig. 8A).

#### 624 *Inhibition of MEK pro-apoptotic signals improves myoblast* 625 *survival*

626 We found that by inhibiting Ras/MEK-mediated pro-apoptotic  
 627 signals in activating satellite cells under our relatively benign  
 628 culture conditions, we could protect on average one satellite  
 629 cell per myofibre from apoptosis (~15% of the satellite cell  
 630 population) (Fig. 8A). We predicted that this modest improve-  
 631 ment in satellite cell survival should subsequently be reflected  
 632 in a proportionate increase in the number of amplifying  
 633 myoblast progeny. To confirm this, EDL myofibre preparations  
 634 were maintained in 10% serum-containing medium in the  
 635 continuous presence of MEK inhibitor plus BrdU for 24 h,  
 636 during the period of satellite cell activation. The myofibres  
 637 were then washed and maintained for a further 24 h (until T48)  
 638 in 10% serum without BrdU or inhibitor. To disassociate any  
 639 effects of proliferation from survival, some preparations were  
 640 fixed after the initial 24 h and anti-BrdU immunostaining  
 641 confirmed that MEK inhibition did not cause premature entry

642 into the cell cycle (both control and MEK-treated myofibres  
 643 had 1 BrdU+ cell per 10 myofibres). Pax7 immunostaining  
 644 revealed that temporary inhibition of MEK between T0 and T24  
 645 significantly increased ( $P < 0.05$ ) the average number of myo-  
 646 blasts per myofibre that survived to T48 (14 cells/fibre,  
 647  $n = 19$  fibres), compared to controls (10 cells/fibre,  $n = 20$  fibres;  
 648 Fig. 8B). From our knowledge of satellite cell proliferation  
 649 kinetics in vitro [4], two cell doublings should have occurred by  
 650 T48. Thus, the extra four myoblasts per fibre is fully consistent  
 651 with the protection of on average one satellite cell per  
 652 myofibre during the activation phase.

## 553 Discussion

554 Previous studies have reported that erbB2, erbB3 and erbB4  
 555 receptors are expressed by normal adult skeletal muscles  
 556 exclusively at the NMJ [25,26], while erbB1–erbB3 receptors  
 557 have been detected on differentiating myoblasts in vitro  
 558 [21,31–33]. However, the expression of erbB receptors by  
 559 myogenic cells during the intervening period, at the onset of  
 560 muscle regeneration, has hitherto not been explored. Here, we  
 561 provide the first description that erbB1–4 receptor tyrosine  
 562 kinases and NRDC co-receptor become expressed by satellite  
 563 cells, the stem cell population of adult skeletal muscle, as they  
 564 activate from quiescence. Signals transduced via erbB recep-  
 565 tors control a diverse set of cellular functions, from growth,  
 566 migration and differentiation, to survival and apoptosis [22].  
 567 Within myoblasts, the functions attributed to erbB signalling  
 568 include neuregulin/erbB3-mediated promotion of differentia-  
 569 tion and fusion [33] and erbB2-dependent survival of differ-  
 570 entiating myoblasts [21]. Specifically, erbB2 conditional  
 571 knockout mice have been created, in which the muscle  
 572 creatine kinase promoter (MCK) drives Cre-mediated excision  
 573 of floxed erbB2 exclusively in heart and skeletal muscles [21].  
 574 These erbB2-deficient mice exhibit extensive myoblast apop-  
 575 tosis during differentiation [21]. However, MCK is not  
 576 expressed by undifferentiated satellite cells [58] and only  
 577 becomes expressed during myoblast differentiation [21], so  
 578 the role of erbB2 during the early stages of muscle regenera-  
 579 tion could not be assessed in that model.

680 Using the isolated myofibre culture system, an in vitro  
 681 model of satellite cell activation, we have found that although  
 682

683 absent during quiescence, erbB receptors can be detected on  
684 satellite cells after 6 h of culture under activating conditions.  
685 This is well before cell division occurs in this model system [10]  
686 and so erbB signalling cannot play a significant role in cell  
687 proliferation or differentiation at this stage. Instead, our results  
688 suggest that signalling via erbB2, and to a lesser extent via  
689 erbB1, provides an anti-apoptotic survival mechanism for  
690 satellite cells undergoing activation; a process that normally  
691 occurs in the context of a damaged, degenerating muscle  
692 environment. Sequential staining experiments indicate that  
693 erbB1 and erbB2 are phosphorylated co-ordinately in >80% of  
694 satellite cells at T24, although this may not necessarily be in the  
695 form of erbB1/erbB2 heterodimers. It is unclear what functions  
696 erbB3 and erbB4 might serve in activated satellite cells. Canto et  
697 al. [29,59] show that erbB3 and erbB4 signalling are important  
698 for glucose transport in skeletal muscle, although it is not  
699 known whether satellite cells are involved. We found that  
700 inhibition of erbB3 between T24 and T48 did not promote  
701 caspase-8-mediated apoptosis, although the number of MyoD+  
702 cells was lower than controls, suggesting a possible role in  
703 promoting cell proliferation or a return to quiescence. The role  
704 of erbB4 signalling is not explored directly in this paper. ErbB4  
705 is detectable from T24 onwards on satellite cells and it could be  
706 operating in the form of erbB4/erbB2 heterodimers. However, it  
707 is clear that NRG, an important erbB4 ligand, is insufficient by  
708 itself to promote satellite cell survival even though it was used  
709 at a concentration (71 ng/ml) that should maximise receptor  
710 stimulation (ED<sub>50</sub> 0.5–2.0 ng/ml, R&D Systems data sheet).

711 In serum-free conditions, a mixture of three erbB ligands  
712 (NRG, EGF and HB-EGF) was found to reduce caspase-8  
713 activation in myoblasts and to help preserve myoblast cell  
714 numbers, although it remains to be proven if this link is  
715 causal. These erbB ligands were specifically chosen because  
716 they are produced by skeletal muscle [60–62], and it is  
717 therefore likely that these growth factors would be readily  
718 available to satellite cells following myotrauma. Despite the  
719 likely availability of erbB ligand growth factors, only a  
720 subpopulation of satellite cells were found to be using erbB1  
721 or erbB2 signalling at any one time during activation. Thus, by  
722 T24, about 3 satellite cells per myofibre robustly express erbB1  
723 and have the receptor in a phosphorylated state; while all  
724 satellite cells express erbB2 by T24, although only about 2  
725 satellite cells per myofibre have erbB2 in a phosphorylated  
726 state. These values are consistent with our observation that  
727 between T0 and T24 about one satellite cell per myofibre  
728 (~15% of the quiescent population) is protected from apopto-  
729 sis by erbB2 signalling. In the presence of increased oxidative  
730 stress (100 μM H<sub>2</sub>O<sub>2</sub>), a closer analogy to in vivo myotrauma  
731 and ischemia-reperfusion injuries [12–14,19,63], an additional  
732 two satellite cells per myofibre (~45% of the population) are  
733 protected from cell death by erbB2 signalling.

734 In a variety of cell types, ROS stimulates erbB1 phosphory-  
735 lation [64,65], and because erbB1 activation can transactivate  
736 erbB2 [22,66,67], it follows that those satellite cells under the  
737 greatest pro-apoptotic stress should exhibit the highest activity  
738 of erbB1/erbB2. If the anti-apoptotic signals are removed, by  
739 inhibiting erbB2 phosphorylation using AG825, then these cells  
740 become overwhelmed by pro-apoptotic signals and die.

741 The pro-apoptotic and anti-apoptotic mechanisms that  
742 operate in activating satellite cells are most likely complex

and interactive. Nevertheless, erbB signalling modules are 743  
well placed to be important master regulators of these 744  
signalling networks. Thus, erbB receptor signalling directly 745  
activates Ras/Raf/MAP-K, PI3-K/Akt, PLCγ/PKC and STAT 746  
signal transduction pathways. All of these root pathways 747  
can subsequently affect the survival/apoptosis balance of the 748  
cell, although the details are cell-type dependent and some- 749  
times contradictory [54]. Moreover, the apoptotic process can 750  
feed back on erbB signalling, since several caspases cleave 751  
erbB1 and erbB2 [54,68]. 752

Our data indicate an anti-apoptotic role for STAT3 within 753  
activating satellite cells. STAT3 becomes potently activated in 754  
satellite cells within 3 h of myotrauma [69] and induces the 755  
transcription of anti-apoptotic Bcl-2/x and caspase inhibitors 756  
[54], the latter being consistent with our observation of a large 757  
increase in caspase-8 activation following STAT3 inhibition. 758  
Because erbB1–erbB2 heterodimers directly phosphorylate 759  
STAT3 [53], any erbB1/2 signalling is likely to provide a crucial 760  
source of phosphorylated STAT3 to help maintain the viability 761  
of a stressed satellite cell. 762

Conversely, our data suggest a pro-apoptotic role for MEK 763  
within activating satellite cells. Little is known concerning the 764  
role of MEK in apoptosis, although interestingly one report 765  
demonstrates that inhibition of MEK1,2 prevents apoptosis in 766  
a lung cancer cell line [70]. We find that inhibition of MEK1,2 767  
phosphorylation preserves on average one satellite cell per 768  
myofibre, subsequently resulting in a proportionate increase 769  
in the numbers of proliferating myoblast progeny. Co-inhibi- 770  
tion of MEK and erbB2 prevents the loss of satellite cells 771  
normally seen with erbB2 inhibition alone. The different 772  
outcomes of MEK inhibition and MEK/erbB2 dual-inhibition 773  
would be consistent with a model whereby erbB2 signals act to 774  
prevent apoptosis initiation, while MEK signals promote 775  
apoptosis execution. Although our data suggests direct 776  
intracellular links between erbB1/2 signalling and apoptotic 777  
pathways in satellite cells, we cannot exclude the possibility 778  
that erbB1/2 activation initiates a cascade of extracellular 779  
signalling between satellite cells and the parent myofibre that 780  
then indirectly leads to the initiation of apoptosis within the 781  
satellite cell. For instance, cleavage of erbB2 by caspase-8 in 782  
MCF7 cancer cells results in their increased susceptibility to 783  
the pro-apoptotic inflammatory cytokine TNF-α [68,71], also 784  
expressed within muscle following reperfusion injury [72]. 785

From a therapeutic perspective, our data suggest that 786  
inhibitors of erbB2 activity, such as the anti-cancer drug 787  
Herceptin, may have unforeseen adverse effects on skeletal 788  
muscle regeneration; while prompt and acute inhibition of MEK 789  
following muscle damage could protect at least 15% of satellite 790  
cells from cell death, thereby increasing the overall efficiency of 791  
adult skeletal muscle regeneration. These results may also 792  
have relevance both for muscle wasting diseases such as 793  
cachexia [73]; and for muscular dystrophy, characterised by 794  
repeated rounds of muscle degeneration and regeneration. 795

## Acknowledgments

We thank Peter Zammit for comments on the manuscript. 798  
This work was funded by the MRC and by the MYORES 799  
Network of Excellence (contract 511978) from the European 800

801 Commission 6th Framework Programme. JPG is funded by an  
802 MRC Collaborative Career Development Fellowship in Stem  
803 Cell Research.

## 80 4 REFERENCES

- 805  
806 [1] A. Mauro, Satellite cell of skeletal muscle fibers, *J. Biophys.*  
807 *Biochem. Cytol.* 9 (1961) 493-495.
- 808 [2] F.P. Moss, C.P. Leblond, Satellite cells as the source of nuclei in  
809 muscles of growing rats, *Anat. Rec.* 170 (1971) 421-435.
- 810 [3] C.A. Collins, I. Olsen, P.S. Zammit, L. Heslop, A. Petrie, T.A.  
811 Partridge, J.E. Morgan, Stem cell function, self-renewal, and  
812 behavioral heterogeneity of cells from the adult muscle  
813 satellite cell niche, *Cell* 122 (2005) 289-301.
- 814 [4] P.S. Zammit, L. Heslop, V. Hudon, J.D. Rosenblatt,  
815 S. Tajbakhsh, M.E. Buckingham, J.R. Beauchamp, T.A.  
816 Partridge, Kinetics of myoblast proliferation show that  
817 resident satellite cells are competent to fully regenerate  
818 skeletal muscle fibers, *Exp. Cell Res.* 281 (2002) 39-49.
- 819 [5] S.S. Jejurikar, W.M. Kuzon Jr., Satellite cell depletion in  
820 degenerative skeletal muscle, *Apoptosis* 8 (2003) 573-578.
- 821 [6] P.M. Siu, E.E. Pistilli, D.C. Butler, S.E. Alway, Aging influences  
822 cellular and molecular responses of apoptosis to skeletal  
823 muscle unloading, *Am. J. Physiol.: Cell Physiol.* 288 (2005)  
824 C338-C349.
- 825 [7] M.C. Kamradt, F. Chen, S. Sam, V.L. Cryns, The small heat  
826 shock protein alpha B-crystallin negatively regulates  
827 apoptosis during myogenic differentiation by inhibiting  
828 caspase-3 activation, *J. Biol. Chem.* 277 (2002) 38731-38736.
- 829 [8] K. Dee, M. Freer, Y. Mei, C.M. Weyman, Apoptosis coincident  
830 with the differentiation of skeletal myoblasts is delayed by  
831 caspase 3 inhibition and abrogated by MEK-independent  
832 constitutive Ras signaling, *Cell Death Differ.* 9 (2002) 209-218.
- 833 [9] Z. Yablonka-Reuveni, A.J. Rivera, Temporal expression of  
834 regulatory and structural muscle proteins during myogenesis  
835 of satellite cells on isolated adult rat fibers, *Dev. Biol.* 164  
836 (1994) 588-603.
- 837 [10] P.S. Zammit, J.P. Golding, Y. Nagata, V. Hudon, T.A. Partridge,  
838 J.R. Beauchamp, Muscle satellite cells adopt divergent fates:  
839 A mechanism for self-renewal? *J. Cell Biol.* 166 (2004)  
840 347-357.
- 841 [11] A.C. Wozniak, J. Kong, E. Bock, O. Pilipowicz, J.E. Anderson,  
842 Signaling satellite-cell activation in skeletal muscle: markers,  
843 models, stretch, and potential alternate pathways, *Muscle*  
844 *Nerve* 31 (2005) 283-300.
- 845 [12] L. Zuo, T.L. Clanton, Reactive oxygen formation in the  
846 transition to hypoxia in skeletal muscle, *Am. J. Physiol.: Cell*  
847 *Physiol.* (2005).
- 848 [13] M. Stangel, U.K. Zettl, E. Mix, J. Zielasek, K.V. Toyka, H.P.  
849 Hartung, R. Gold, H<sub>2</sub>O<sub>2</sub> and nitric oxide-mediated oxidative  
850 stress induce apoptosis in rat skeletal muscle myoblasts,  
851 *J. Neuropathol. Exp. Neurol.* 55 (1996) 36-43.
- 852 [14] V. Adams, S. Gielen, R. Hambrecht, G. Schuler, Apoptosis in  
853 skeletal muscle, *Front. Biosci.* 6 (2001) D1-D11.
- 854 [15] M. Benhar, D. Engelberg, A. Levitzki, ROS, stress-activated  
855 kinases and stress signaling in cancer, *EMBO Rep.* 3 (2002)  
856 420-425.
- 857 [16] D. Caporossi, S.A. Ciafre, M. Pittaluga, I. Savini, M.G. Farace,  
858 Cellular responses to H<sub>2</sub>O<sub>2</sub> and bleomycin-induced  
859 oxidative stress in L6C5 rat myoblasts, *Free Radical Biol. Med.*  
860 35 (2003) 1355-1364.
- 861 [17] V. Renault, L.E. Thornell, G. Butler-Browne, V. Mouly, Human  
862 skeletal muscle satellite cells: aging, oxidative stress and the  
863 mitotic clock, *Exp. Gerontol.* 37 (2002) 1229-1236.
- 864 [18] S. Fulle, S. Di Donna, C. Puglielli, T. Pietrangelo, S. Beccafico, R.  
865 Bellomo, F. Protasi, G. Fano, Age-dependent imbalance of the  
antioxidative system in human satellite cells, *Exp. Gerontol.* 40 (2005) 189-197.
- [19] L.L. Ji, C. Leeuwenburgh, S. Leichtweis, M. Gore, R. Fiebig, J.  
Hollander, J. Bejma, Oxidative stress and aging. Role of  
exercise and its influences on antioxidant systems, *Ann. N. Y.*  
*Acad. Sci.* 854 (1998) 102-117.
- [20] M. Horikawa, S. Higashiyama, S. Nomura, Y. Kitamura, M.  
Ishikawa, N. Taniguchi, Upregulation of endogenous  
heparin-binding EGF-like growth factor and its role as a  
survival factor in skeletal myotubes, *FEBS Lett.* 459 (1999)  
100-104.
- [21] E.R. Andrecke, W.R. Hardy, A.A. Girgis-Gabardo, R.L. Perry, R.  
Butler, F.L. Graham, R.C. Kahn, M.A. Rudnicki, W.J. Muller,  
ErbB2 is required for muscle spindle and myoblast cell  
survival, *Mol. Cell. Biol.* 22 (2002) 4714-4722.
- [22] T. Holbro, N.E. Hynes, ErbB receptors: directing key signaling  
networks throughout life, *Annu. Rev. Pharmacol. Toxicol.* 44  
(2004) 195-217.
- [23] E. Nishi, A. Prat, V. Hospital, K. Elenius, M. Klagsbrun,  
N-arginine dibasic convertase is a specific receptor for  
heparin-binding EGF-like growth factor that mediates cell  
migration, *EMBO J.* 20 (2001) 3342-3350.
- [24] M.D. Marmor, K. Bose Skaria, Y. Yarden, Signal transduction  
and oncogenesis by ErbB/HER receptors, *Int. J. Radiat. Oncol.*  
*Biol. Phys.* 58 (2004) 903-913.
- [25] X. Zhu, C. Lai, S. Thomas, S.J. Burden, Neuregulin receptors,  
erbB3 and erbB4, are localized at neuromuscular synapses,  
*EMBO J.* 14 (1995) 5842-5848.
- [26] J.C. Trinidad, G.D. Fischbach, J.B. Cohen, The Agrin/MuSK  
signaling pathway is spatially segregated from the  
Neuregulin/ErbB receptor signaling pathway at the  
neuromuscular junction, *J. Neurosci.* 20 (2000) 8762-8770.
- [27] S.A. Jo, X. Zhu, M.A. Marchionni, S.J. Burden, Neuregulins are  
concentrated at nerve-muscle synapses and activate  
ACh-receptor gene expression, *Nature* 373 (1995) 158-161.
- [28] N. Altiok, J.L. Bessereau, J.P. Changeux, ErbB3 and ErbB2/neu  
mediate the effect of heregulin on acetylcholine receptor  
gene expression in muscle: differential expression at the  
endplate, *Embo J.* 14 (1995) 4258-4266.
- [29] C. Canto, E. Suarez, J.M. Lizcano, E. Grino, P.R. Shepherd, L.G.  
Fryer, D. Carling, J. Bertran, M. Palacin, A. Zorzano, A. Guma,  
Neuregulin signaling on glucose transport in muscle cells,  
*J. Biol. Chem.* 279 (2004) 12260-12268.
- [30] P. Fumagalli, M. Accarino, A. Egeo, P. Scartezzini, G. Rappazzo,  
A. Pizzuti, V. Avvantaggiato, A. Simeone, G. Arrigo, O.  
Zuffardi, S. Ottolenghi, R. Taramelli, Human NRD convertase:  
a highly conserved metalloendopeptidase expressed at  
specific sites during development and in adult tissues,  
*Genomics* 47 (1998) 238-245.
- [31] B.D. Ford, B. Han, G.D. Fischbach, Differentiation-dependent  
regulation of skeletal myogenesis by neuregulin-1, *Biochem.*  
*Biophys. Res. Commun.* 306 (2003) 276-281.
- [32] J.M. Harper, P.J. Buttery, Effects of EGF receptor ligands on  
fetal ovine myoblasts, *Domest. Anim. Endocrinol.* 20 (2001)  
21-35.
- [33] D. Kim, S. Chi, K.H. Lee, S. Rhee, Y.K. Kwon, C.H. Chung, H.  
Kwon, M.S. Kang, Neuregulin stimulates myogenic  
differentiation in an autocrine manner, *J. Biol. Chem.* 274  
(1999) 15395-15400.
- [34] R. Kelly, S. Alonso, S. Tajbakhsh, G. Cossu, M. Buckingham,  
Myosin light chain 3F regulatory sequences confer  
regionalized cardiac and skeletal muscle expression in  
transgenic mice, *J. Cell Biol.* 129 (1995) 383-396.
- [35] S. Tajbakhsh, E. Bober, C. Babinet, S. Pournin, H. Arnold, M.  
Buckingham, Gene targeting the myf-5 locus with nlacZ  
reveals expression of this myogenic factor in mature skeletal  
muscle fibres as well as early embryonic muscle, *Dev. Dyn.*  
206 (1996) 291-300.
- [36] J.D. Rosenblatt, A.I. Lunt, D.J. Parry, T.A. Partridge, Culturing

- 935 satellite cells from living single muscle fiber explants, *In Vitro*  
 936 *Cell Dev. Biol., Anim.* 31 (1995) 773-779.
- 937 [37] A. Levitzki, A. Gazit, Tyrosine kinase inhibition: an approach  
 938 to drug development, *Science* 267 (1995) 1782-1788.
- 939 [38] N. Osherov, A. Gazit, C. Gilon, A. Levitzki, Selective inhibition  
 940 of the epidermal growth factor and HER2/neu receptors by  
 941 tyrophostins, *J. Biol. Chem.* 268 (1993) 11134-11142.
- 942 [39] E. Hamada, T. Nishida, Y. Uchiyama, J. Nakamura, K. Isahara,  
 943 H. Kazuo, T.P. Huang, T. Momoi, T. Ito, H. Matsuda, Activation  
 944 of Kupffer cells and caspase-3 involved in rat hepatocyte  
 945 apoptosis induced by endotoxin, *J. Hepatol.* 30 (1999) 807-818.
- 946 [40] J. Turkson, D. Ryan, J.S. Kim, Y. Zhang, Z. Chen, E. Haura, A.  
 947 Laudano, S. Sebti, A.D. Hamilton, R. Jove, Phosphotyrosyl  
 948 peptides block Stat3-mediated DNA binding activity, gene  
 949 regulation, and cell transformation, *J. Biol. Chem.* 276 (2001)  
 950 45443-45455.
- 951 [41] N.K. Lebrasseur, G.M. Cote, T.A. Miller, R.A. Fielding, D.B.  
 952 Sawyer, Regulation of neuregulin/ErbB signaling by  
 953 contractile activity in skeletal muscle, *Am. J. Physiol.: Cell*  
 954 *Physiol.* 284 (2003) C1149-C1155.
- 955 [42] J.R. Beauchamp, L. Heslop, D.S. Yu, S. Tajbakhsh, R.G. Kelly, A.  
 956 Wernig, M.E. Buckingham, T.A. Partridge, P.S. Zammit,  
 957 Expression of CD34 and Myf5 defines the majority of  
 958 quiescent adult skeletal muscle satellite cells, *J. Cell Biol.* 151  
 959 (2000) 1221-1234.
- 960 [43] T. Joh, M. Itoh, K. Katsumi, Y. Yokoyama, T. Takeuchi, T. Kato,  
 961 Y. Wada, R. Tanaka, Physiological concentrations of human  
 962 epidermal growth factor in biological fluids: use of a  
 963 sensitive enzyme immunoassay, *Clin. Chim. Acta* 158 (1986)  
 964 81-90.
- 965 [44] S. Chakrabarty, S. Huang, T.L. Moskal, H.A. Fritsche Jr.,  
 966 Elevated serum levels of transforming growth factor-alpha in  
 967 breast cancer patients, *Cancer Lett.* 79 (1994) 157-160.
- 968 [45] S.E. Bastian, A.J. Dunbar, I.K. Priebe, P.C. Owens, C. Goddard,  
 969 Measurement of betacellulin levels in bovine serum,  
 970 colostrum and milk, *J. Endocrinol.* 168 (2001) 203-212.
- 971 [46] L.M. Gilmour, K.G. Macleod, A. McCaig, J.M. Sewell, W.J.  
 972 Gullick, J.F. Smyth, S.P. Langdon, Neuregulin expression,  
 973 function, and signaling in human ovarian cancer cells, *Clin.*  
 974 *Cancer Res.* 8 (2002) 3933-3942.
- 975 [47] M. Kruidering, G.I. Evan, Caspase-8 in apoptosis: the  
 976 beginning of "the end"? *IUBMB Life* 50 (2000) 85-90.
- 977 [48] S.H. Kaufmann, M.O. Hengartner, Programmed cell death:  
 978 alive and well in the new millennium, *Trends Cell Biol.* 11  
 979 (2001) 526-534.
- 980 [49] S. Zhuang, M.C. Lynch, I.E. Kochevar, Caspase-8 mediates  
 981 caspase-3 activation and cytochrome c release during singlet  
 982 oxygen-induced apoptosis of HL-60 cells, *Exp. Cell Res.* 250  
 983 (1999) 203-212.
- 984 [50] D.S. Lidke, P. Nagy, R. Heintzmann, D.J. Arndt-Jovin, J.N. Post,  
 985 H.E. Grecco, E.A. Jares-Erijman, T.M. Jovin, Quantum dot  
 986 ligands provide new insights into erbB/HER  
 987 receptor-mediated signal transduction, *Nat. Biotechnol.* 22  
 988 (2004) 198-203.
- 989 [51] D. Graus-Porta, R.R. Beerli, J.M. Daly, N.E. Hynes, ErbB-2,  
 990 the preferred heterodimerization partner of all ErbB recep-  
 991 tors, is a mediator of lateral signaling, *EMBO J.* 16 (1997)  
 992 1647-1655.
- 993 [52] F. McArdle, S. Spiers, H. Aldemir, A. Vasilaki, A. Beaver, L.  
 994 Iwanejko, A. McArdle, M.J. Jackson, Preconditioning of  
 995 skeletal muscle against contraction-induced damage: the role  
 996 of adaptations to oxidants in mice, *J. Physiol.* 561 (2004)  
 997 233-244.
- 998 [53] A. Fernandes, A.W. Hamburger, B.I. Gerwin, ErbB-2  
 999 kinase is required for constitutive stat 3 activation in  
 1000 malignant human lung epithelial cells, *Int. J. Cancer* 83 (1999)  
 1001 564-570.
- 1002 [54] A.J. Danielsen, N.J. Maihle, The EGF/ErbB receptor family and  
 1003 apoptosis, *Growth Factors* 20 (2002) 1-15.
- [55] X. Liu, K. Ye, Src homology domains in phospholipase  
 C-gamma1 mediate its anti-apoptotic action through  
 regulating the enzymatic activity, *J. Neurochem.* 93 (2005)  
 892-898.
- [56] X.T. Wang, K.D. McCullough, X.J. Wang, G. Carpenter, N.J.  
 Holbrook, Oxidative stress-induced phospholipase C-gamma  
 1 activation enhances cell survival, *J. Biol. Chem.* 276 (2001)  
 28364-28371.
- [57] T. Mutoh, T. Kumano, H. Nakagawa, M. Kuriyama, Role of  
 tyrosine phosphorylation of phospholipase C gamma1 in  
 the signaling pathway of HMG-CoA reductase  
 inhibitor-induced cell death of L6 myoblasts, *FEBS Lett.* 446  
 (1999) 91-94.
- [58] G. Ferrari, G. Salvatori, C. Rossi, G. Cossu, F. Mavilio, A  
 retroviral vector containing a muscle-specific enhancer  
 drives gene expression only in differentiated muscle fibers,  
*Hum. Gene Ther.* 6 (1995) 733-742.
- [59] C. Canto, A.V. Chibalin, B.R. Barnes, S. Glund, E. Suarez, J.W.  
 Ryder, M. Palacin, J.R. Zierath, A. Zorzano, A. Guma,  
 Neuregulins mediate calcium-induced glucose transport  
 during muscle contraction, *J. Biol. Chem.* 281 (2006)  
 21690-21697.
- [60] J.A. Abraham, D. Damm, A. Bajardi, J. Miller, M. Klagsbrun,  
 R.A. Ezekowitz, Heparin-binding EGF-like growth factor:  
 characterization of rat and mouse cDNA clones, protein  
 domain conservation across species, and transcript  
 expression in tissues, *Biochem. Biophys. Res. Commun.* 190  
 (1993) 125-133.
- [61] L. Frati, G. Cenci, G. Sbaraglia, D.V. Teti, I. Covelli, Levels of  
 epidermal growth factor in mice: tissues measured by a  
 specific radioreceptor assay, *Life Sci.* 18 (1976)  
 905-911.
- [62] M. Hiramatsu, M. Kashimata, F. Takayama, K. Tsubakida,  
 K. Ri, N. Minami, Reduced level of epidermal growth factor in  
 the skeletal muscle of mice with muscular dystrophy, *Horm.*  
*Metab. Res.* 24 (1992) 138-139.
- [63] B.B. Rubin, G. Chang, S. Liauw, A. Young, A. Romaschin, P.M.  
 Walker, Phospholipid peroxidation deacylation and  
 remodeling in postischemic skeletal muscle, *Am. J. Physiol.*  
 263 (1992) H1695-H1702.
- [64] Y. Fang, S.I. Han, C. Mitchell, S. Gupta, E. Studer, S. Grant, P.B.  
 Hylemon, P. Dent, Bile acids induce mitochondrial ROS, which  
 promote activation of receptor tyrosine kinases and signaling  
 pathways in rat hepatocytes, *Hepatology* 40 (2004)  
 961-971.
- [65] K. Takeyama, K. Dabbagh, J. Jeong Shim, T. Dao-Pick, I.F. Ueki,  
 J.A. Nadel, Oxidative stress causes mucin synthesis via  
 transactivation of epidermal growth factor receptor: role of  
 neutrophils, *J. Immunol.* 164 (2000) 1546-1552.
- [66] R. Goldman, R.B. Levy, E. Peles, Y. Yarden, Heterodimerization  
 of the erbB-1 and erbB-2 receptors in human breast  
 carcinoma cells: a mechanism for receptor transregulation,  
*Biochemistry* 29 (1990) 11024-11028.
- [67] C.R. King, I. Borrello, F. Bellot, P. Comoglio, J. Schlessinger, Egf  
 binding to its receptor triggers a rapid tyrosine  
 phosphorylation of the erbB-2 protein in the mammary  
 tumor cell line SK-BR-3, *EMBO J.* 7 (1988) 1647-1651.
- [68] V. Benoit, A. Chariot, L. Delacroix, V. Derogowski, N. Jacobs,  
 M.P. Merville, V. Bours, Caspase-8-dependent HER-2 cleavage  
 in response to tumor necrosis factor alpha stimulation is  
 counteracted by nuclear factor kappaB through c-FLIP-L  
 expression, *Cancer Res.* 64 (2004) 2684-2691.
- [69] K. Kami, E. Senba, In vivo activation of STAT3 signaling in  
 satellite cells and myofibers in regenerating rat skeletal  
 muscles, *J. Histochem. Cytochem.* 50 (2002) 1579-1589.
- [70] T.T. Nguyen, E. Tran, T.H. Nguyen, P.T. Do, T.H. Huynh, H.  
 Huynh, The role of activated MEK-ERK pathway in  
 quercetin-induced growth inhibition and apoptosis in A549  
 lung cancer cells, *Carcinogenesis* 25 (2004) 647-659.

- 1073 [71] S.S. Jejurikar, E.A. Henkelman, P.S. Cederna, C.L. Marcelo, M.G. 1079  
1074 Urbanchek, W.M. Kuzon Jr., Aging increases the susceptibility 1080  
1075 of skeletal muscle derived satellite cells to apoptosis, Exp. 1081  
1076 Gerontol. (2006). 1082  
1077 [72] F. Zhang, E.C. Hu, J. Gerzenshtein, M.P. Lei, W.C. Lineaweaver, 1083  
1078 The expression of proinflammatory cytokines in the rat 1084  
1085 muscle flap with ischemia-reperfusion injury, Ann. Plast. 1079  
Surg. 54 (2005) 313-317. 1080  
[73] J.E. Belizario, M.J. Lorite, M.J. Tisdale, Cleavage of caspases-1, 1081  
-3, -6, -8 and -9 substrates by proteases in skeletal muscles 1082  
from mice undergoing cancer cachexia, Br. J. Cancer 84 (2001) 1083  
1135-1140. 1084

UNCORRECTED PROOF